ARTICLE

Effects of Plasticization and Shear Stress on Phase Structure Development and Properties of Soy Protein Blends

Feng Chen[†,‡] **and Jinwen Zhang***[,†]

Materials Science Program & Composite Materials and Engineering Center, Washington State University, Pullman, Washington 99164-1806, United States

ABSTRACT In this study, soy protein concentrate (SPC) was used as a plastic component to blend with poly(butylene adipate-co-terephthalate) (PBAT). Effects of SPC plasticization and blend composition on its deformation during mixing were studied in detail. Influence of using water as the major plasticizer and glycerol as the co-plasticizer on the deformation of the SPC phase during mixing was explored. The effect of shear stress, as affected by SPC loading level, on the phase structure of SPC in the blends was also investigated. Quantitative analysis of the aspect ratio of SPC particles was conducted by using ImageJ software, and an empirical model predicting the formation of percolated structure was applied. The experimental results and the model prediction showed a fairly good agreement. The experimental results and statistic analysis suggest that both SPC loading level and its water content prior to compounding had significant influences on development of the SPC phase structure and were correlated in determining the morphological structures of the resulting blends. Consequently, physical and mechanical properties of the blends greatly depended on the phase morphology and PBAT/SPC ratio of the blends.

KEYWORDS: soy protein blend • bioplastics • percolation

1. INTRODUCTION

Biobased polymeric materials have received great attention from both general public and plastic industry itself. Soy protein (SP), the residue from oil crushing of soybean, has been attempted by researchers as a standing-alone (named "neat" thereafter), melt-processable polymer material (1−5), a plastic component in blending (6−8), and a simple filler in various polymer matrices (9−11). The strong intra- and intermolecular interactions of SP make its melt processing very difficult unless a large amount of plasticizer, usually water, and/or glycerol, is present. For melt processing of SP, sodium sulfate is often used to break the intramolecular disulfide bonds and to assist unfolding of the polypeptide chains (12, 13). Processing of neat SP plastic or SP as a plastic component in blending is complicated, considering several changes on the molecular level of SP including gelation (14), plasticization (1, 3, 6), chain unfolding (15, 16), and intermolecular crosslinking (6, 17, 18). Water is the most effective plasticizer and indispensible in melt processing of SP. In addition, glycerol is also recognized as an effective plasticizer for SP (1, 3, 15), but it alone can not make neat SP melt processable. However, neat SP plastics have some intrinsic problems such as poor processability, brittleness, and water/moisture sensitivity. Blending SP with other hydrophobic thermoplastic polymers is the most economic approach to overcome many problems associated with neat SP plastics. SP has been blended with biobased polymers such as poly (lactic acid) (8, 19, 20). However, such SP blends tend to be brittle due to the brittleness of both the biobased polymer and SP itself. To overcome this problem, various synthetic biodegradable polymers which are soft and high ductile, have been used to blend with SP, including poly(butylene succinate-*co*-adipate) (10), polycaprolactone (10, 21), poly(hydroxyl ester ether) (11), and poly(butylene adipate-*co*-terephthalate) (PBAT) (6, 7). Among these polymers, PBAT is readily available at relatively low production cost.

Recently, we demonstrated processing SP as a plastic component in blend compounding with other thermoplastic polymers (6−8, 19, 20). Water was indispensable for SP being a plastic component during compounding, though its content in the formulated SPC prior to compounding (designated "pre-compounding SPC" thereafter) was generally much lower than that needed for melt processing of neat SP. Water played a determining role in plastic deformation of the SP phase during mixing (6). Increasing water content in the pre-compounding SPC greatly enhanced the deformability of the SPC phase and eventually resulted in finer SPC thread structure. Formation of percolated SPC network structure was noted in many thus prepared blends. Therefore, superior overall properties of the polymer blends were obtained by processing SP as plastic instead of as filler (6, 8, 19). It was further demonstrated that the deformability of the SPC phase increased with SPC loading level, as seen from the finer and more stretched SPC threads (7). It should be mentioned that because of the limited amount of water

* Corresponding author. Tel.: 509-335-8723. Fax: 509-335-5077. E-mail: jwzhang@wsu.edu.

Received for review August 17, 2010 and accepted October 4, 2010

† Washington State University.

‡ Pacific Northwest National Laboratory, Richland, Washington 99352, United States.

DOI: 10.1021/am100751c

Published on Web 10/21/2010

and/or glycerol in the pre-compounding SPC, the SPC phase was not in a true melt state during compounding as the neat SP was melt processed under high water and/or glycerol level (1, 22). The plastic behavior of SPC in this case was mainly due to the deformability of plasticized SPC under high shear field in the twin-screw extruder.

It is generally recognized that during mixing the droplets of the dispersed phase are deformed and stretched into filaments by the flow field to the point where they reach a critical diameter, and the filament break-up follows when the stresses generated by flow field can not overcome the surface tension of the droplets formed (23, 24). The deformability of the dispersed phase and shear stress exerted on the dispersed phase have important influences on this deformation process. For SP, its deformability is mainly manipulated by plasticization. Nevertheless, the final morphology of polymer blends, including the size, shape, aggregation, and orientation of the dispersed phase, is complexly influenced by composition, interfacial tension, time of mixing, shear stress, elasticity of the components, and viscosity ratio (25−27).

The major objective of this study was to elucidate the influences of the plasticization of SP phase and the shear stress in compounding process on development of phase morphology of PBAT/SPC blends. In this study, a series of PBAT/SPC blends with varying SPC loading levels and different water contents in the pre-compounding SPC was prepared by extrusion compounding and the test specimens were prepared by injection molding. The morphological structure and mechanical, dynamic mechanical and rheological properties of the resulting blends were studied. The dependences of aspect ratio of SPC domain on water content in pre-compounding SPC and SPC content in the blend were investigated. The correlation between water content in pre-compounding SPC and SPC content in the blends on morphological structure and mechanical properties of the blends was also examined.

2. EXPERIMENTAL SECTION

Materials. SPC (Arcon F) was provided by ADM (Decatur, IL), and contained ca. 69% protein (on dry weight basis), 19% carbohydrate, 3% fat, 7.5 wt % moisture, and small amount of minerals as received. PBAT (Ecoflex F BX 407) was purchased from BASF (Florham Park, NJ), having a weight-average molecular weight of 71.7 kDa and polydispersity of 1.60. Maleic anhydride (MA) (95%) was purchased from Aldrich. MA grafted PBAT (PBAT-g-MA) was prepared by reactive extrusion using dicumyl peroxide 98% as initiator, and the residual MA was removed under high vacuum at 80°C (28). The degree of grafting was 1.40 wt % as determined by titration method (29).

Preparations of Blends and Test Specimens. SP was first formulated containing the following ingredients: SPC (100 parts, on the basis of dry weight), sodium sulfite (0.5 parts), glycerol (10 parts) and/or water. Three levels of water content in the SPC powder were selected: 0.6 wt % (vacuum dried at 70°C for 12 h), 7.5 wt % (native, as received) and 22.5 wt % (by adding 15% extra water to the native SPC), respectively. The formulated SPC was mixed using a kitchen blender, then stored in sealed plastic bags and left overnight at room temperature to equilibrate. The mixture of the formulated SPC, PBAT and PBAT-g-MA was compounded using a co-rotating twin-screw extruder (Leistriz ZSE-18) equipped with 18 mm screws having an L/D ratio of 40. All blends contained 3 parts by weight of PBAT-g-MA, which was used as compatibilizer and replaced an equal amount of neat PBAT in the formulation. The resulting blends are named thereafter "PBAT/X%SPC-Y%H_2O". Utilizing this nomenclature, X denotes the weight percentage of SPC (on dry weight basis) in the blends and Y the water content in pre-compounding SPC. The screw speed was maintained at 80 rpm for all runs, and the eight controlled temperature zones from the first heating zone to the die adaptor were set at 99, 110, 145, 145, 145, 145, 145, and 140 °C, respectively. The residence time was ca. 2 min during extrusion compounding. The extrudate was cooled in a water bath and subsequently granulated by a strand pelletizer. Pellets were exposed in the air for 4 h to further evaporate the residual surface moisture and then dried in a convection oven at 90 °C for more than 12 h (the residual moisture was less than 1%). Test specimens were prepared by a Sumitomo injection molding machine (SE 50D) with barrel zone temperatures set at 155, 160, 160, and 155 °C from the feeding section to the nozzle. Mold temperature was set at 50 °C and cooling time was ca. 30 s. All samples were conditioned for 1 week at 23 ± 2 °C and 50 ± 5% RH prior to mechanical test and characterizations.

Rheology Tests. Dynamic rheological properties of the PBAT/SPC blends were measured using a strain-controlled rheometer (Rheometric Scientific, RDA III) with a parallel-plate geometry (d = 25 mm). The gap distance between the parallel plates was 1 mm for all tests. A strain sweep test was initially conducted to determine the linear viscoelastic region of the materials, then a dynamic frequency sweep test (strain, 3%, frequency, 0.01−500 rad/s) was performed at 160°C. All test samples were cut from the injection molded specimens after conditioning. Because the moisture content of the specimen after conditioning was tested as ca. 1%, no additional protection was taken during the test.

The static melt viscosity of the blends was measured using an Advanced Capillary Extrusion Rheometer ACER 2000 (Rheometric Inc., USA) with a barrel diameter of 20 mm and die length-to-diameter ratio of 15. The shear rate was ranged from 25 to 2000 s^{-1}, and the temperature was set at 160 °C. Sufficient time was set at each shear rate to guarantee the steady state of the polymer melt.

Tensile Test. Tensile tests were performed on an 8.9 kN, screw-driven universal testing machine (Instron 4466) equipped with a 10 kN electronic load cell and machine grips. The tests were conducted at a crosshead speed of 5 mm/min with strain measured using a 25 mm extensometer (MTS 634.12 × 10^{-24}). All tests were carried out according to the ASTM standard and 5 replicates were tested for each sample to obtain an average value. All samples were tested after one week of conditioning at 23 ± 2 °C and 50 ± 5% RH.

Microscopy. Field-emission scanning electron microscopy (FE SEM, Quanta 200F) was utilized to investigate the SPC phase structure, the SPC phase was isolated by removing the PBAT phase with extraction. The PBAT phase in the blends was removed by Soxhlet extraction using $CHCl_3$, and the sample was wrapped in a pouch of filter paper to minimize the disturbance of the SPC phase by the solvent flow. The isolated SPC was gently suspended in $CHCl_3$ and spin coated onto mica slices at low speed limit. The unprocessed SPC particles were also suspended in $CHCl_3$ and spin coated in the same way. All FE SEM specimens were sputter coated with gold prior to examination.

Image Analysis. ImageJ software was used to measure the aspect ratio of the extracted SPC phase on the FE SEM images. Approximately 30 images including ca. 400 pieces of SPC filaments/particles were measured and calculated to obtain the average aspect ratio of SPC phase in blends.

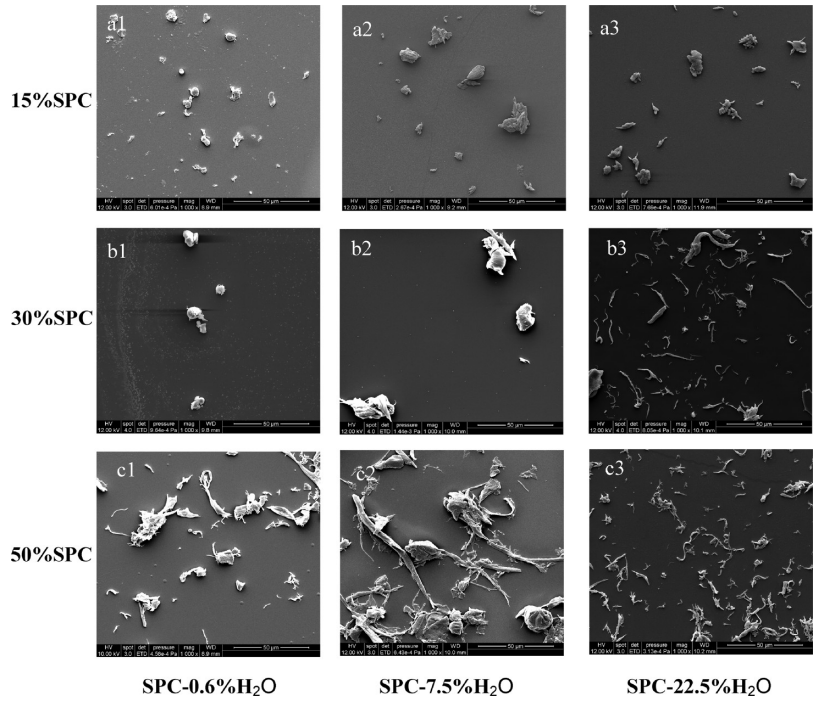

FIGURE 1. FE SEM micrographs showing the influences of SPC loading level and water content in pre-compounding SPC on the SPC phase morphology. PBAT/SPC ratio (w/w): (a) 85/15; (b) 70/30; and (c) 50/50. Water content in pre-compounding SPC: 0.6% (a1, b1, and c1), 7.5% (a2, b2, and c2), and 22.5% (a3, b3, and c3). SPC was isolated after the complete removal of PBAT by Soxhlet extraction using $CHCl_3$ and then spin-coated on mica slice for observation.

Dynamic Mechanical Analysis. Dynamic mechanical properties were measured by a dynamic mechanical analyzer (DMA, Rheometrics Solids Analyzer, RSAII). DMA specimens (12.6× 3.2×35 mm^3) were cut from the injection molded samples and conditioned in the same environment as tensile samples. DMA testing was conducted on a dual-cantilever fixture at a frequency of 1 Hz. Strain sweep tests were performed on each sample to determine the linear viscoelastic region. All tests were conducted at a strain of 0.03% using a 2 °C/min temperature ramp from −45 to 110 °C. The weight loss of specimen through the DMA test was measured to be ca. 1% for all samples, which could be approximately assumed as the residual moisture and volatiles in the SPC phase.

Statistical Data Analysis. Minitab statistical software package (Minitab 15) was used to examine the effect of water content in pre-compounding SPC and SPC content as well as their interactions on the mechanical properties of PBAT/SPC blends, applying a two way interaction fixed effects model. The confidence level was set as 95%. Five replicates of each blend specimen were tested. The normal distribution and constant variance assumptions of the model were checked by normal probability plot and residuals vs fits plot. Tukey method with 95% confidence level was used to perform the multiple comparisons among the levels of one factor (water content or SPC content) with the other factor (SPC content or water content) fixed.

3. RESULTS AND DISCUSSION

3.1. Development of SPC Phase Structure in Blends. Mixing of two immiscible polymer melts involves deformation of the dispersed droplets and break-up. The droplet deformation is promoted by the shear stress (τ) exerted by the flow field but resisted by the interfacial stress (σ/R), where σ is the surface tension and R is the local radius of the droplet. The ratio of the two stresses, named the capillary number (30), Ca, determines whether the droplet phase will disperse or remain stable within the flow field.

$$Ca = \tau R/\sigma \quad (1)$$

When the local radius R of the droplet is large during the initial stages of mixing, the interfacial stress σ/R is overwhelmed by the shear stress, hence resulting in stable deformation of the droplets into threads. The dispersive mixing (break-up of the threads) will occur when the diameter of the threads is reduced to a level that the capillary number approaches a critical value, Ca_{crit}, at which point the interfacial stress starts to compete with shear stress. On the other hand, the break-up time strongly depends on the viscosity ratio (31, 32). The residence time within a given deformation process must be sufficiently long to allow break-up to occur. It is widely observed that low viscosity ratio (especially when viscosity ratio $\lambda = \eta_d/\eta_m < 1$) favored the break-up of droplets (30). Therefore, the driving force for droplet deformation is shear stress which is promoted by melt viscosity, whereas the rate of droplet deformation achievable depends on λ, and interfacial tension (σ) tends to coalesce the droplet and retain the spherical shape therefore resisting the deformation (30, 32−35).

In this work, water was used as the major plasticizer and influence of its loading level on phase structure development of SPC was studied. Glycerol was used as a co-plasticizer and its loading level was fixed at 10%. Figure 1 shows that as the water content in the pre-compounding SPC increased from 0.6 to 22.5%, PBAT/SPC blends with different SPC loading levels behaved differently in the evolution of SPC

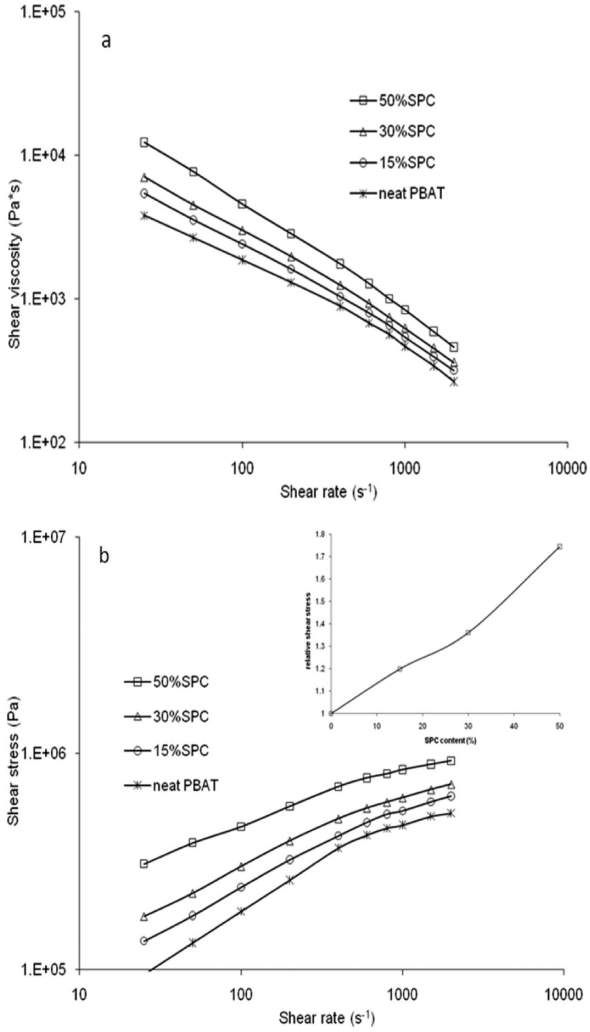

FIGURE 2. (a) Melt shear viscosity and (b) shear stress of PBAT/SPC blends with different SPC loading levels and extreme water contents in pre-compounding SPC. The inset is shear stress relative to that of neat PBAT at shear rate of 2000 s^{-1}.

phase morphology. At a low SPC loading level, i.e., at the PBAT/SPC ratio of 85/15 (w/w), SPC was mainly in particulate form and displayed minimum stretching and reduction in size irrespective of water content in the pre-compounding SPC. During pre-compounding, a PBAT/SPC ratio of 70/30 (w/w), the SPC phase structure strongly depended on water content. At a high SPC loading level, i.e., PBAT/SPC = 50/50 (w/w), however, significant deformation and stretching of SPC were seen at all levels of water content. Clearly, the phase structure of the SPC domains depended on both water content in the pre-compounding SPC and PBAT/SPC ratio, and these two variables appeared to be correlated. Since all blends were compatibilized using the same amount of PBAT-g-MA, the interfacial tension between PBAT and SPC phases might be approximately assumed at the same level. Therefore, the deformation of the SPC phase with varying SPC loading level and water content in the pre-compounding SPC was attributed to the combined influence of shear stresses exerted on SPC in compounding process and SPC/PBAT viscosity ratio.

Because water served as an excellent plasticizer for SPC, higher water content in the pre-compounding SPC was expected to result in lower viscosity of SPC in the compounding process. It is important to note that SPC was not able to form an ideal melt with this relatively low plasticizer concentrations in the study, hence its viscosity could not be practically measured or imitated using a rheometer. Therefore the SPC viscosity or SPC/PBAT viscosity ratio refers only to qualitative comparison. In other words, it might be more appropriate to suggest that the SPC formulated with more water had higher deformability during mixing. Traditional rheology of filled and multiphase systems both predict that the melt viscosity gradually increases with increasing filler volume fraction in the low filler concentration range and tremendously escalates at high filler concentrations (36). Corresponding to the increase in viscosity, the shear stress increases as well. The shear stress on SPC exerted by the melt was not drastically increased in the case of 15% SPC with respect to that of neat PBAT. Without sufficient shear stress imposed by the melt, the SPC particle was unable to deform even though it contained high water content. Further increase in shear stress became noticeable at 30% SPC. When SPC loading level reached 50%, the shear stress was large enough to severely deform the more rigid SPC (with 0.6% water).

This reasoning is supported by the apparent melt viscosity and shear stress of the blends under different shear rates. Figure 2a shows the shear viscosity vs shear rate for the blends prepared from the dried SPC (PBAT/SPC-0.6% H_2O), and Figure 2b gives the corresponding shear stress in melt flow field. The inset in Figure 2b show the relative shear stress in the flow filed with respect to that of the neat PBAT at shear rate of 2000 s^{-1}, a level of shear rate that the melt easily experiences in twin-screw extrusion. With 15% SPC, the shear stress of the blends was ~1.2 times that of neat PBAT (Figure 2b). It seems that such an increase was not

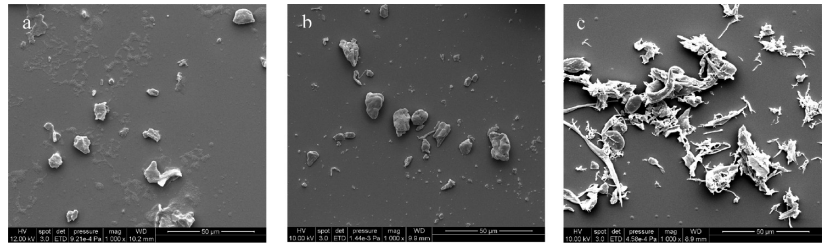

FIGURE 3. FE SEM micrographs showing the influence of glycerol on the SPC phase morphology in the PBAT/SPC (50/50 w/w) blends. The SPC was vacuum dried at 80°C for 8h and the residual moisture content was ca. 0.6% before compounding with PBAT. (a) Unprocessed SPC as received; (b) without glycerol; (c) with glycerol.

enough to cause large deformation of the SPC phase even when SPC contained a relatively high level of plasticizer (22.5% H_2O and 10% glycerol). For the blends with 30% SPC, shear stress in flow field further increased to ~1.35 times that of the neat PBAT, which resulted in increasing deformation of the SPC domains with water content. At the level of 50% SPC, the shear stress of flow field was increased to ~1.8 times that of the neat PBAT. Under this high shear condition, the SPC with low water content (0.6% H_2O) was also forced to undertake large deformation.

Water and glycerol are often used together to plasticize SP in the literature (1, 8). The deformability of dried SPC at the loading level of 50% was due to the presence of 10% glycerol on the basis of SPC weight. As shown in Figure 3, compared with the unprocessed SPC, the dried SPC without the addition of glycerol at the same loading level behaved like rigid filler in the matrix (Figures 3a and b). However, the addition of 10 wt % glycerol to this dried SPC enabled the SPC phase significant deformability at the PBAT/SPC ratio of 50/50 (w/w) as reflected in size reduction and stretching of the SPC domains during compounding (Figure 3c).

3.2. Dynamic Rheological Properties. Although SPC was processed as a plastic component during compounding, the resulting PBAT/SPC compounds were more like in situ formed composites (6, 7). Extensive cross-linking of soy protein that occurred during compounding (6) and most water evaporating after drying produced the elastic modulus of SPC phase at ca. 12 times that of the neat PBAT. Consequently, the SPC phase became too rigid to be easily deformed in the following process and behaved more like fillers in the matrix polymer. Dynamic rheological properties are very sensitive to structure and interactions within the polymer melt (37−39). Figure 4 compares the dynamic rheological properties of PBAT/SPC blends prepared from dried SPC (ca. 0.6% moisture) and SPC containing 22.5% water, respectively. For the neat PBAT melt, the logarithmic storage (G') and loss (G'') moduli versus logarithmic frequency (ω) demonstrated a typical polymer melt behavior, showing a smooth linear relationship by $G' \propto \omega^{1.75}$ and $G'' \propto \omega^{0.94}$ in the terminal (low-frequency) zone. The addition of rigid filler to a neat polymer generally results in significant increases in elastic properties and relaxation times (40). In dynamic rheology testing, such increases are especially manifested in the deviation of viscoelastic response of the blends in the terminal zone from that of the neat polymer. In Figure 4, both G' and G'' of the blends increased with SPC content, and this increase became more pronounced in the terminal zone. The blends prepared from SPC containing 22.5% water exhibited larger G' and G'' than the corresponding blends prepared from dried SPC. Similar changes were also noted in the static melt viscosities of these blends (Figure 2). Because the solid structure of a material can be preserved under small-strain testing, the slopes of log(G') and log(G'') vs. log(ω) in the terminal zone, which is an indicator for the frequency dependences of G' and G'', are often used to assess the morphological structure for composites. In

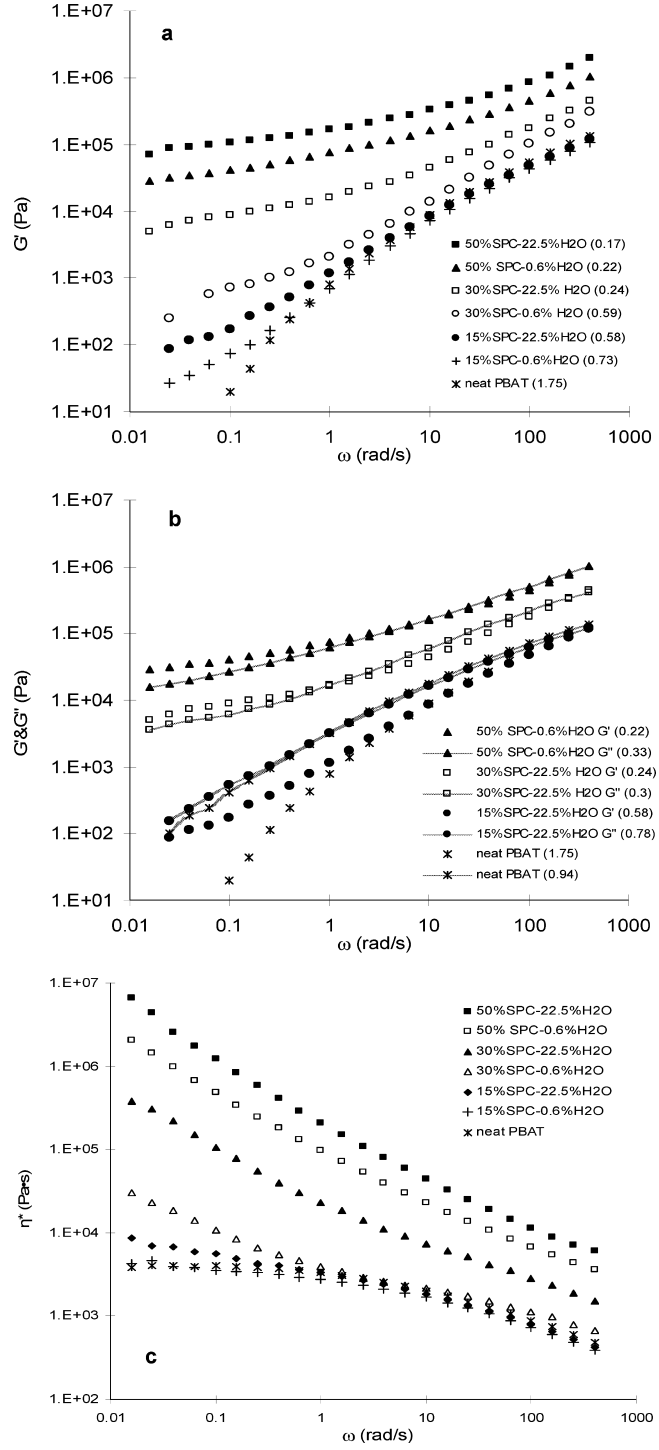

FIGURE 4. Effects of composition and water content in pre-compounding SPC on dynamic rheological behavior of PBAT/SPC blends. Two extreme water levels, 0.6 and 22.5%, were chosen for comparison. Strain = 3%, temperature = 160°C.

Figure 4, both G' and G'' in the terminal zone became less frequency dependent (showing smaller slope) as SPC content in the blend and water content in pre-compounding SPC increased, respectively, i.e., displaying enhanced pseudo-solid-like behavior of the melt.

The log(G') vs. log(ω) of PBAT/15% SPC-0.6% H_2O, PBAT/15% SPC-22.5% H_2O, and the PBAT/30% SPC-0.6% H_2O blends exhibited similar terminal slope values (0.58−0.73)

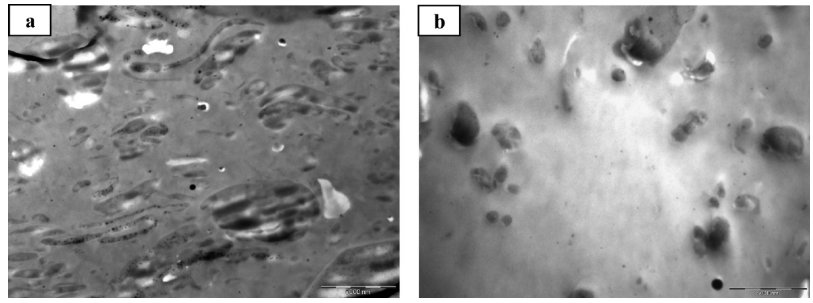

FIGURE 5. TEM micrographs of the PBAT/SPC blends for (a) PBAT/50 % SPC-0.6 % H_2O and (b) PBAT/15 % SPC-22.5 % H_2O. The scale bar represented 5000 nm.

which departed greatly from that of the neat PBAT but still suggested significant frequency dependence of G'. This dynamic rheological behavior was typical for the homogeneously filled polymer melt. In contrast, the PBAT/50 % SPC-0.6 % H_2O, PBAT/50 % SPC-22.5 % H_2O, and the PBAT/30 % SPC-22.5 % H_2O blends demonstrated much lower slope values (0.17−0.24), and the log(G') vs. log(ω) curves in the terminal zone tended to become flat ("secondary plateau"). In this case, the weak dependence of G′ on frequency was a strong indication of pseudo-solid-like behavior of the melt in the terminal region. Further indication of such behavior was the higher G' than G'' for these blends in the terminal region (Figure 4b). This strong pseudo-solid-like behavior of the melt suggests the existence of solid network structure in these blends and the fact that water content in pre-compounding SPC and SPC content were two important factors influencing the formation of such structure. The crossover of G′ and G″ for these blends at higher frequencies was likely due to the disruption of the percolated SPC structure under high shear stress (7). On the other hand, the melts of the PBAT/15 % SPC, PBAT/30 % SPC-0.6 % H_2O and PBAT/30 % SPC-7.5 % H_2O blends (not shown in Figure 4b), whose G' showed significant dependence on ω in the terminal region, all exhibited a higher G'' than G' in the whole frequency range of test as neat PBAT, suggesting SPC was in a dispersed state in these blends. Figure 5 also clearly shows the influence of SPC loading level (hence flow field shear stress) on morphological structures of the blends. At 50 % SPC, the shear stress was high enough that even the dried SPC (ca. 0.6 % H_2O) could be deformed, and the stretched SPC thread formed percolated structures. At 15 % SPC, however, the relatively low shear stress was not able to sufficiently deform the SPC phase even though SPC contained 22.5 % H_2O, and SPC was homogenously dispersed as particulates in the matrix. Corresponding to the changes in G′ and G″, complex viscosity of the blends in the terminal zone quickly deviated from Newtonian (primary) plateau of the neat PBAT and became more shear-thinning with increasing SPC content or water content (Figure 4c), demonstrating more solidlike behavior for blends with high SPC content or high water level in the pre-compounding SPC. The results of rheological properties were consistent with the morphological evidence as shown in Figure 1.

3.3. Percolated SPC Network Structure and Tensile Mechanical Properties of the Blends. For a polymer blend or composite system, percolation describes a state of continuity in which the particles of the minor phase touch each other by ends. According to Willemse et al. (41), the percolation threshold value is the onset limit of volume fraction for the continuity of the minor phase, and not all particles of the minor phase are a necessary part of the percolated structure at the threshold point. With continuous increase in volume fraction, more minor phase particles will incorporate into the percolating structure until at a certain volume fraction where all the particles touch one another and become part of a single percolating structure. In other words, a co-continuous structure is obtained. That volume fraction, also named maximum packing density (ϕ_{max}), is of great interest because it is the onset point for many properties such as mechanical, rheological and electric (if applicable) properties to display drastic changes. Numerous studies have demonstrated that ϕ_{max} is a function of size and shape of the dispersed phase (41−46). The following empirical equation relating ϕ_{max} of randomly oriented rods to their aspect ratios L/B was introduced by Cross et al. (42), and further applied by Willemse (41).

$$\frac{1}{\phi_{max}} = 1.38 + 0.0376\left(\frac{L}{B}\right)^{1.4} \qquad (2)$$

Here L is the length and B is the diameter of the particle.

Table 1 gives the average L/B ratios of the SPC particles in each blend and the corresponding ϕ_{max} calculated using the above model. SPC particles became more elongated with either higher SPC loading level or higher water content in the pre-compounding SPC. For the PBAT/SPC (50/50 w/w) blends, the SPC volume fraction (0.485) was higher than the ϕ_{max} value for the SPC particles in blends with different water levels, suggesting SPC particles reached fully percolation state in all cases. For the PBAT/SPC (85/15 w/w) blends, however, the result indicates that SPC particles were unable to form an effective percolated structure in the blends. For the PBAT/SPC (70/30 w/w) blends, the volume fraction (0.287) was lower than the ϕ_{max} value (0.41) for the SPC particles in the PBAT/30 % SPC-7.5 % H_2O blend but higher than the ϕ_{max} value for the SPC particles in the PBAT/30 % SPC-22.5 % H_2O blend. This result suggests that at the 30 % SPC loading level, full percolation would be achieved with pre-compounding SPC with a water level falling between 7.5 and 22.5 %, which was in agreement with our previous study of the effect of water content on SPC percolation structure in the PBAT/SPC (70/30 w/w) blends (6).

Table 1. Number Average Local *L*/*B* Ratio of the SPC Phase in the Blends

PBAT/SPC blends						tensile properties		
weight ratio	ϕ_{SPC}[a]	H_2O% in pre-compounding SPC		SPC thread *L*/*B* ratio	ϕ_{max}[b]	modulus (MPa)	strength(MPa)	elongation (%)
85/15		0.6	F[c]	1.93 ± 0.3	0.678	158 ± 10	13.4 ± 0.2	451 ± 24.1
	0.142	7.5	FG	2.5 ± 1.5	0.658	156 ± 6	13.3 ± 0.0	437 ± 20.1
		22.5	GH	2.8 ± 0.6	0.649	156 ± 4	14.0 ± 0.1	408 ± 25.9
70/30		0.6	D	1.87 ± 0.3	0.68	274 ± 17	11.0 ± 0.1	80.5 ± 6.5
	0.287	7.5	D	10.8 ± 1.4	0.41	287 ± 10	11.2 ± 0.1	64.6 ± 5.8
		22.5	E	20.0 ± 2.3	0.257	411 ± 48	19.3 ± 0.6	40.1 ± 5.2
50/50		0.6	A	11.6 ± 1.1	0.394	659 ± 18	14.2 ± 0.4	8.0 ± 1.4
	0.485	7.5	B	18.1 ± 1.5	0.282	765 ± 56	19.2 ± 0.6	11.0 ± 1.0
		22.5	C	34.8 ± 4.6	0.147	937 ± 77	24.5 ± 0.7	11.6 ± 1.6

[a] ϕ_{SPC} was the experimental SPC volume fraction calculated on the basis of the SPC weight percentage, the density of PBAT and the density of SPC (ca. 1.35 g/cm^3) (47). [b] $\phi_{max}$is calculated from eq 2, basing on a specific SPC aspect ratio to form percolated structure. [c] Minitab software and Tukey multiple comparison of water content effect on the yield stresses of PBAT/SPC blends with fixed SPC loading level. Water contents with different letters mean their yield stresses are significantly different from each other. The confidence level of statistic analysis was set as 95%.

The mechanical properties of a blend strongly depend on its composition and morphology as well as the geometry of the dispersed domains. The results in Table 1 indicate that elastic modulus experienced great increase while elongation at break decreased rapidly with increasing SPC loading level. On the other hand, with SPC content increased from 15 to 30 wt %, strength showed a slight decrease except for the PBAT/30%SPC-22.5%H_2O blend, which had a percolated SPC structure and exhibited a significantly higher strength. The slightly higher strength of PBAT/15%SPC was probably caused by strain hardening of PBAT which occurred in the high strain region in the late stage of tensile testing. The further increase in strength for the blends with 50 wt % SPC might be primarily attributed to the increase in the aspect ratio of SPC phase and the SPC percolation. The yield properties and modulus are particularly sensitive to variation of aspect ratio of the dispersed phase and the formation of percolated structure. At 30 wt % SPC, modulus, yield stress and strain of the blends demonstrated sudden changes when percolated SPC structure was formed. Because all blends with 50 wt % SPC had a percolated SPC structure, increase in aspect ratio of SPC phase (by increasing water content in the pre-compounding SPC) only led to gradual change in yield properties. In contrast, for the blends with 15 wt % SPC, SPC was basically dispersed as particulate filler (aspect ratio ~1) and no percolation structure was formed; hence the influence of water content in pre-compounding SPC was not obvious (Figure 6).

To further investigate the correlation between the influences of water content in pre-compounding SPC and PBAT/SPC ratio on the phase structure and properties of PBAT/SPC blends, a two-way interaction fixed effects model was applied using yield stress as the response parameter. This is because yield stress is recognized as the parameter that could greatly impact the phase structure of polymer blends. SPC content was set as one factor with 3 levels, 15, 30, and 50%, and water content in pre-compounding SPC was fixed as a secondary factor with 3 levels, 0.6, 7.5, and 22.5%. The confidence level was set as 95%. The response parameter, yield stress, was transformed to the reverse of the value (yield stress^{-1}) because of the violation of the constant variance assumption. The transformed data was tested to meet the assumptions of normal distribution and constant

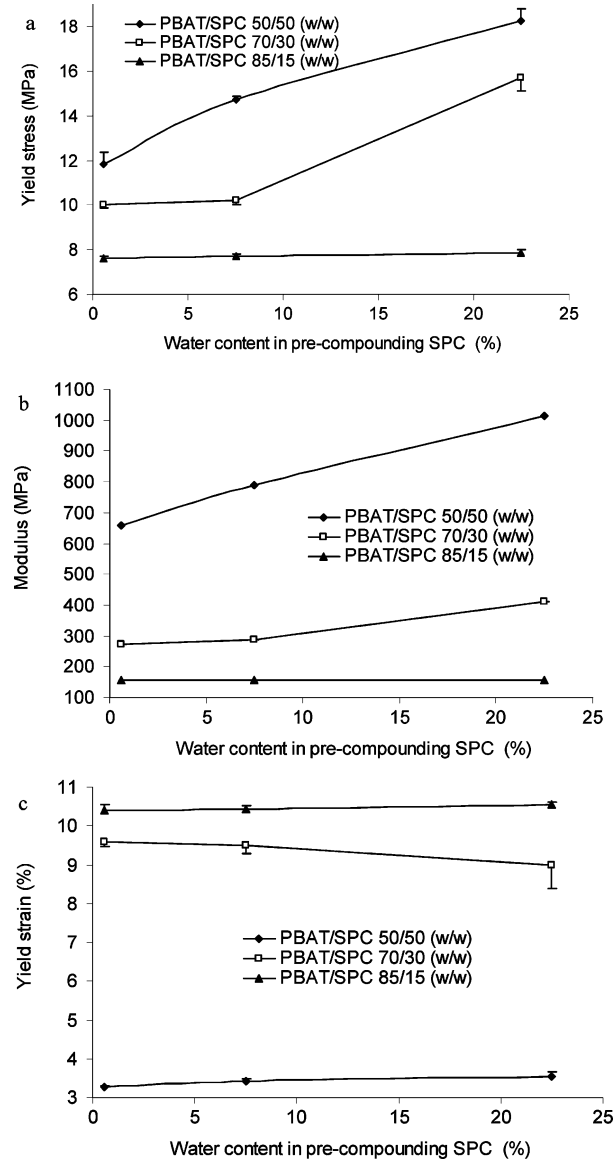

FIGURE 6. Effects of SPC loading level and water content in pre-compounding SPC on the yield properties and modulus of PBAT/SPC blends.

Table 2. Statistical Analysis[a] of the Significances of SPC Loading Level and Water Content in Pre-compounding SPC

	DF	SS	MS	F	P
SPC loading level	2	0.0292062	0.0146031	5286.97	<0.001
water content in pre-compounding SPC	2	0.0042419	0.0021210	767.88	<0.001
interaction[b]	4	0.0019799	0.0004950	179.21	<0.001
error	36	0.0000994	0.0000028		
total	44	0.0355274			

[a] Performed on the Minitab software. [b] Two-way interaction fixed effects model.

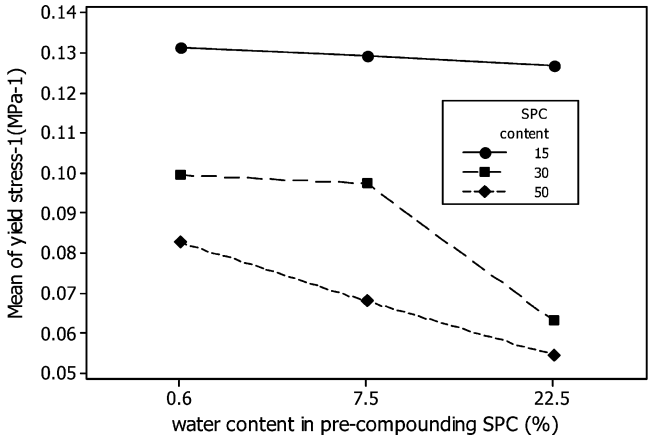

FIGURE 7. Plot of interaction showing the significance of the interaction between SPC loading level and water content in pre-compounding SPC on the mechanical properties of PBAT/SPC blends.

variance. Both the p-value ($p < \alpha = 0.05$) in Table 2 and the nonparallel interaction plot of minitab output (Figure 7) reveals the significance of the interaction between water content effect and SPC content effect. The mean values of yield stresses in the blocked factor SPC content were 7.74, 12.06, and 15.07 MPa for 15, 30 and 50% SPC, respectively; suggesting the influence of water content on the mechanical properties of PBAT/SPC blends was stronger in the blends with higher SPC content. This result was verified by the Tukey multicomparison with fixed levels of SPC content, as shown in Table 1. Different labeling letters represented significant differences in yield stress. Hence, the effect of water content in pre-compounding SPC on mechanical properties of the blends depended on the blend composition. However, at all SPC levels, higher water content in pre-compounding SPC manifested more noticeable effect on the mechanical properties of the resulting blends.

3.4. Dynamic Mechanical Analysis. Dynamic mechanical properties of PBAT/SPC blends also depended on composition of the blends and water content in the pre-compounding SPC. In Figure 8, neat PBAT displayed a major damping peak at −15.5 °C, which was attributed to the α-transition of the aliphatic polyester segments of PBAT (48). A similar observation was reported in our previous study (7). All the PBAT/SPC blends demonstrated a similar α-transition with almost identical peak temperatures to that of neat PBAT, suggesting SPC was not miscible with PBAT. Because SPC was in glassy state and had low damping in this temperature range (8), the peak height of the α-transition of PBAT in blends was substantially lower than that of the neat PBAT and continuously decreased with increasing SPC loading level. The further reduction in the height of damping peak with increasing water content in pre-compounding was probably due to the formation of finer SPC threads that could more effectively inhibit the movement of PBAT molecular chains (7). Neat PBAT also showed a weak transition around 60°C as seen in the small hump in the damping curve and an associated decrease in storage modulus (E'). This transition was attributed to the α-transition of the aromatic segments in PBAT (7, 48). It is interesting to note that the damping of the blends increased with SPC content at temperatures above 65°C. This increase was most likely attributed to the broad α-transition of SPC (with 10% glycerol and certain residual H_2O), which fell in this range (8).

Figure 8 also shows that E' of the blends increased with both SPC loading level and water content in the pre-compounding SPC. If it isassumed that the storage modulus

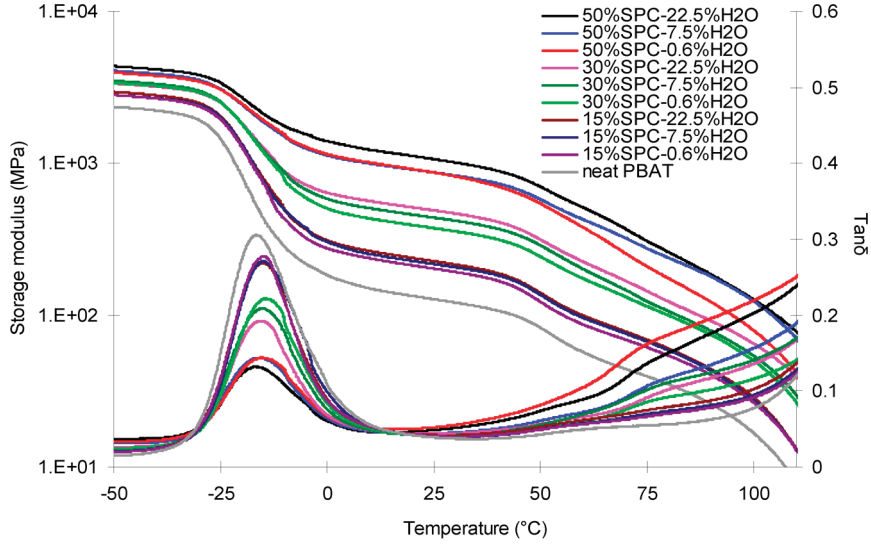

FIGURE 8. Effects of SPC content and water content on dynamical mechanical properties of PBAT/SPC blends.

of a composite could be also qualitatively described by a general composite model, e.g., Halpin and Tsai model which takes into account factors such as geometry of the filler and relative moduli of the filler and matrix, such change in E' is reasonably understandable. Because E′ of neat SPC was much higher than that of neat PBAT and SPC was in the glassy state within a large part of the testing temperature range (1, 7), E' of the blends was noted to increase with the SPC loading level. In addition, the finer SPC phase structure resulted from high water content would further enhance the E' value.

4. CONCLUSIONS

During blending SPC with PBAT, the plasticization of SPC and composition of blend both had great influences on the deformation of SPC phase and the morphology of the resulting blends. Water and glycerol were both good plasticizers for SPC in terms of increasing SPC plasticity. Plasticization was necessary for SPC to be processed as a plastic component in blending with other polymers. When SPC was not plasticized, for example in the case of dried SPC without addition of glycerol, the dried SPC (contained ~0.6% H_2O) basically functioned as a filler and showed little evidence of plastic deformation after mixing. When SPC contained 10% glycerol and was loaded at a level of 50%, even the dried SPC demonstrated significant deformability during mixing and presented as stretched threads. The deformability of SPC during mixing increased progressively with water content in pre-compounding SPC. However, the phase structure of SPC was not only determined by its plasticization but also its loading level, which in turn greatly influenced the shear stress in the flow field. For example, at the 15% loading level, even well plasticized with 22.5% H_2O, the SPC displayed little plastic deformation after blending. In contrast, at the 30% loading level, the same plasticized SPC experienced great plastic deformation. Clearly, water content in pre-compounding SPC and SPC loading level correlated in determining the phase structure of the resulting blends, i.e., less plasticizer was required for SPC to undergo similar deformation at higher SPC loading level. Percolated SPC network structure was formed under certain circumstances, depending on the amount of plasticizer (water) and blend composition. The percolation structure of SPC in the blends could also be predicted by an empirical model developed by Cross, and the prediction from the model agreed well with the experiment results.

Acknowledgment. The authors are grateful for the financial supports from the National Research Initiative of the USDA Cooperative State Research, Education and Extension Service, grant number 2007-35504-17818, and from the United Soybean Board (USB).

REFERENCES AND NOTES

(1) Zhang, J.; Mungara, P.; Jane, J. *Polymer* **2001**, *42*, 2569–2578.
(2) Wang, N.; Zhang, L. *Polym. Int.* **2005**, *54*, 233–239.
(3) Chen, P.; Zhang, L. *Macromol. Biosci.* **2005**, *5*, 237–245.
(4) Mo, X.; Sun, X. *J. Polym. Environ.* **2003**, *11*, 15–22.
(5) Sun, X.; Kim, H.; Mo, X. *J. Am. Oil Chem. Soc.* **1999**, *76*, 117–123.
(6) Chen, F.; Zhang, J. *Polymer* **2009**, *50*, 3770–3777.
(7) Chen, F.; Zhang, J. *Polymer* **2010**, *51*, 1812–1819.
(8) Zhang, J.; Jiang, L.; Zhu, L.; Jane, J.; Mungara, P. *Biomacromolecules* **2006**, *7*, 1551–1561.
(9) Zhong, Z.; Sun, X. *J. Appl. Polym. Sci.* **2003**, *88*, 407–413.
(10) John, J.; Bhattacharya, M. *Polym. Int.* **1999**, *48*, 1165–1172.
(11) Wang, C.; Carriere, C. J.; Willett, J. L. *J. Polym. Sci. Part B: Polym. Phys.* **2002**, *40*, 2324–2332.
(12) Shimada, K.; Cheftel, J. C. *J. Agric. Food Chem.* **1989**, *37*, 161–168.
(13) Jane, J. L.; Wang, S. U.S. Patent 5 523 293, 1996.
(14) Hermansson, A. M. *J. Am. Oil Chem. Soc.* **1986**, *63*, 658–666.
(15) Mo, X.; Sun, X. *J. Am. Oil Chem. Soc.* **2002**, *79*, 197–202.
(16) Kitabatake, N.; Tahara, M.; Doi, E. *Agric. Biol. Chem.* **1990**, *54*, 2205–2212.
(17) Wu, Q.; Zhang, L. *Ind. Eng. Chem. Res.* **2001**, *40*, 1879–1883.
(18) Park, S. K.; Bae, D. H.; Rhee, K. C. *J. Am. Oil Chem. Soc.* **2000**, *77*, 879–884.
(19) Liu, B.; Jiang, L.; Liu, H.; Sun, L.; Zhang, J. *Macromol. Mater. Eng.* **2010**, *295*, 123–129.
(20) Liu, B.; Jiang, L.; Liu, H.; Zhang, J. *Ind. Eng. Chem. Res.* **2010**, *49*, 6399–6406.
(21) Zhong, Z.; Sun, XS. *Polymer* **2001**, *42* (16), 6961–69.
(22) Ralston, B. E.; Osswald, T. A. *J. Polym. Environ.* **2008**, *16*, 169–176.
(23) Sundararaj, U.; Macosko, C. W. *Macromolecules* **1995**, *28*, 2647–2657.
(24) Willemse, R. C.; Ramaker, E. J. J.; Van Dam, J.; Posthuma De Boer, A. *Poly. Eng. Sci.* **1999**, *39*, 1717–1725.
(25) Favis, B. D.; Chalifoux, J. P. *Polymer* **1988**, *29*, 1761–1767.
(26) Favis, B. D. Polymer Blends, Vol. 1: Formulation. Wiley: New York, 2000; p 502.
(27) Tucker, C. L.; Moldenaers, P. *Annu. Rev. Fluid Mech.* **2002**, *34*, 177–210.
(28) Jiang, L.; Huang, J.; Qian, J.; Chen, F.; Zhang, J.; Wolcott, M. P.; Zhu, Y. *J. Polym. Environ.* **2008**, *16*, 83–93.
(29) Lin, C.; Lee, W. *J. Appl. Polym. Sci.* **1998**, *70*, 383–387.
(30) Wilkinson, A.; Ryan, A. *Polymer Processing and Structure Development*; Springer: Dordrecht, 1998; p 207−208.
(31) Janssen, J. M. H.; Meijer, H. E. H. *J. Rheol.* **1993**, *37*, 597–608.
(32) Grace, H. P. *Chem. Eng. Commun.* **1982**, *14*, 225–277.
(33) Tomotika, S. *Proc. R. Soc. London* **1936**, *A153*, 302–318.
(34) Mikami, T.; Cox, R. G.; Mason, S. G. *Int. J. Multiphase Flow* **1975**, *2*, 113–138.
(35) Khakhar, D. V.; Ottino, J. M. *Int. J. Multiphase Flow* **1987**, *13*, 71–86.
(36) Dealy, J. M., Wissbrun, K. F. Melt rheology and its role in plastics processing: theory and applications. Van Nostrand Reinhold: New York, 1990; pp390−391.
(37) Utracki, L. A. *Polymer Alloys & Blends*; Carl Hanser: New York, 1989; p131−174.
(38) Du, M.; Zheng, Q.; Yang, H. *Nihon Reoroji Gakkaishi* **2003**, *31*, 305–311.
(39) Zhang, Q.; Cao, Y.; Du, M. *J. Mater. Sci.* **2004**, *39*, 1813–1814.
(40) Graebling, D.; Muller, R.; Palienme, J. F. *Macromolecules* **1993**, *26*, 320–329.
(41) Willemse, R.; Posthuma de Boer, A.; Van Dam, J.; Gotsis, A. *Polymer* **1998**, *39*, 5879–5887.
(42) Cross, M. M.; Kaye, A.; Stanford, J. L.; Stepto, R. F. *Polym. Mater. Sci. Eng.* **1983**, *49*, 531–535.
(43) Banerjee, P.; Mandal, B. M. *Macromolecules* **1995**, *28*, 3940–3943.
(44) Karásek, L.; Meissner, B.; Asai, S.; Sumita, M. *Polym. J.* **1996**, *28*, 121–126.
(45) Garboczi, E. J.; Snyder, K. A.; Douglas, J. F.; Thorpe, M. F. *Phys. Rev. E* **1995**, *52*, 819–828.
(46) Lyngaae-Jorgensen, J.; Utracki, L. *Mackromol. Chem. Macromol. Symp.* **1991**, *48/49*, 189.
(47) Jong, L. *Composites, Part A* **2006**, *37*, 438–466.
(48) Dacko, P.; Kowalczuk, M.; Janeczek, H.; Sobota, M. *Macromol. Symp.* **2006**, *239*, 209–216.

AM100751C